Journal of Engineering Mathematics **31:** 357–378, 1997.

Coupled transport of multi-component solutes in porous media

MICHAEL SHAPIRO* and [1]PIERRE M. ADLER
Faculty of Mechanical Engineering, Technion – Israel Institute of Technology, Haifa 32000, Israel, [1]*Laboratoire de Phénomènes de Transports dans les Mélanges, CNRS, Asterama 2, Avenue du Téléport, 86360 Chasseneuil du Poitou, France*

Received 23 May 1995; accepted in revised form 23 April 1996

Key words: convective-diffusion, reactive species, macroscale matrix properties, coupling

Abstract. Coupled convective-diffusive transport of multicomponent solutes in spatially-periodic models of porous media is considered. Species coupling at the micro- or interstitial scale results from a first-order irreversible surface reaction on the bed elements, composing the porous medium, and from the off-diagonal terms of the microscale matrix transport coefficients.

The coarse-scale long-time solute matrix properties are calculated, namely, mean effective reactivity, velocity and dispersivity. These coefficients are analyzed in several important particular cases, pertaining to reactive and nonreactive constituents. The solution scheme is illustrated by an example of two reactive solute components with diffusional coupling, flowing in a bundle of tubes model porous medium. The effective matrix axial transport coefficients are analyzed for various values of the dimensionless Damkohler number, *Da*, associated with the surface-reaction constant. Analytical expressions for the effective axial transport properties are obtained in cases of extreme (small and large) values of the dimensionless Damkohler numbers.

The microscale molecular diffusive coupling provides for each solute constituent two diffusive pathways to the reactive tube wall: one – via the direct diffusivity component, another – via the coupling diffusivity. The macroscopic manifestation of this microscale coupling is to give rise to coupling off-diagonal terms in the effective matrix transport coefficients: positive off-diagonal terms in the reactivity matrix and negative off-diagonal terms in velocity and dispersivity matrices. From a physical viewpoint microscale coupling brings about a more uniform solute distribution within the tube cross section, which reduces the effective axial transport.

1. Introduction

In 1953 G.I. Taylor [1] showed that axial dispersion of a solute instantaneously introduced in a Poiseuille flow within a circular capillary tube of radius a may be described by a one-dimensional convective-diffusive equation

$$\frac{\partial \overline{P}}{\partial t} + \overline{U}_{\text{eff}} \frac{\partial \overline{P}}{\partial x} = \overline{D}_{\text{eff}} \frac{\partial^2 \overline{P}}{\partial x^2}, \tag{1}$$

where $\overline{P}$ is the cross-sectionally averaged solute concentration, $\overline{U}_{\text{eff}} = \overline{U}$ is the average flow (solvent) velocity and $\overline{D}_{\text{eff}}$ is the effective, or apparent solute diffusivity in the axial (x) flow direction. For sufficiently long times the effective axial diffusivity is independent of the initial solute distribution and given by

$$\overline{D}_{\text{eff}} = \frac{\overline{U}^2 a^2}{48D}, \tag{2}$$

with D being the solute true molecular diffusivity. This result means that $\overline{D}_{\text{eff}}$ is not a property of the solute, but depends also on the flow rate, tube size, etc. Aris [2] derived a more accurate expression for $\overline{D}_{\text{eff}}$

$$\overline{D}_{\text{eff}} = D + \frac{\overline{U}^2 a^2}{48D} \tag{2a}$$

which, similarly to the Taylor formula (1), is valid for asymptotic long time $t \gg a^2/D$ after the injection of the solute into the flow. Attempts to extend these results for times preceding or comparable to a^2/D showed that $\overline{D}_{\text{eff}}, \overline{U}_{\text{eff}}$ are no longer constants, but, rather, depend in a complicated manner on time and the initial solute distribution [3,4].

The treatments of Taylor and Aris spurred numerous studies of dispersion processes including the effects of cross-sectional tube geometry, external forces [5,6] acting on solute particles, chemical reactions [7,8], surface transport [9], nonspherical particle shape [10], transport in sheared suspensions [11]. These and many other convective dispersion processes may be treated by a general formalism outlined in the Macrotransport Theory [12].

All the above studies dealt with a one-component solute dissolved in a passive flowing solvent. In many circumstances solutes consisting of several components should be treated. When transport of each component is independent of the others, the homogenization problem for each component may be solved independently. A more important case pertains to situations where the transport processes of different components are not independent, but, rather, *coupled*. A notable example is provided by diffusion of heat and mass in multi-component systems. If we consider, for example, transport of two species, diffusing in nonuniform fields of concentration C_1, C_2, and temperature T, then the mass fluxes $\mathbf{j}_k$ $(k = 1, 2)$ and heat flux $\mathbf{j}_T$ are given by [13]:

$$\mathbf{j}_T = D_T \nabla \left(\frac{1}{T}\right) - \frac{1}{T} D_{Ti} \nabla C_i,$$

$$\mathbf{j}_k = D_{kT} \nabla \left(\frac{1}{T}\right) - \frac{1}{T} D_{ki} \nabla C_i, \quad k = 1, 2.$$

In the above D_T and D_{kk} $k = 1, 2$ are related to the thermal conductivity and the species diffusion coefficients, respectively. The coupling coefficients D_{kT} represent thermal diffusion coefficients, which bring about species fluxes due to a temperature gradient even in the absence of externally imposed concentration gradients (Soret effect). Furthermore, D_{Tk} are diffusional thermal-effect coefficients, leading to the appearance of a nonzero heat flux in isothermal systems (Dufour effect). Other coefficients D_{ki} $(k \neq i)$ represent coupling between the component fluxes.

Another example of species coupling of the above type is heat and mass transfer in porous ceramic materials near the pores prevailing in the grain boundary region [14]. External temperature gradient, accompanied by the surface segregation of impurities and/or crystal lattice defects results in a nonzero flux of these substances towards the pore surfaces. These coupled heat and mass-transfer processes significantly affect thermal conductivity of oxide ceramics in vacuum [15].

Coupling also appears when several species undergo heterogeneous catalytic reactions on surfaces of bed (reactor) elements [16]. Here coupling is manifested by dependence of the surface-reaction-conversion rate of one constituent on surface concentration of other constituents. These and other coupled multicomponent systems are abundant in chemical technology [16], hydrology [17], geological applications [18], etc.

The goal of the present paper is to provide a mathematical description of the coupled species transport processes in porous materials, e.g., those envisioned in the above-mentioned applications. Transport in porous environment has been treated in many studies, employing various descriptions of the interstitial porous geometry. The objective of these studies is the calculation of the effective (apparent) transport coefficients suitable for coarse-scale description of transport processes. Towards this goal formulae (2), (2a) of Taylor-Aris were applied to hydrodynamic dispersion in flows through porous materials [19] by means of the bundle-of-tube geometric model [20] to approximate the material geometry. More elaborate geometric models, accounting for the geometric microstructure and tortuous flow pattern prevailing in real materials, can be subdivided into statistical (probabilistic) models [21,22] and deterministic models [23]. The latter have an advantage of accounting for material microstructure by specifying or generating [24] a representative volume element, which adequately reflects the material interstitial geometry. This volume element serves as a unit cell (of a given characteristic size l), which is indefinitely reproduced within the infinite space (see Figure 1). On the coarse scale, L, greatly exceeding the cell size l, solute transport in such lattices may be treated by several techniques [23,25,26], which can be jointly named homogenization methods. The treatment focuses on the calculation of the solute coarse-scale effective transport coefficients (velocity vector $\overline{\mathbf{U}}^*$ and diffusivity dyadic $\overline{\mathbf{D}}^*$), appearing in a three-dimensional version of the transport equation (1). This equation governs the spatially averaged solute concentration $\overline{P}$. The homogenization technique allows to calculate mathematically and rigorously the coarse-scale transport properties, governing solute transport for times $t \gg l^2/D$.

The homogenization methods were also extended for reactive solutes, e.g., those undergoing reactions or phase transitions on surfaces of the bed elements. In this case the coarse-scale equation (1) includes the term $\overline{K}^*\overline{P}$, with $\overline{K}^*$ being the effective volumetric reaction-rate coefficient. The trio of transport coefficients $\overline{\mathbf{U}}^*, \overline{\mathbf{D}}^*, \overline{K}^*$ governing coarse-scale transport of a single reactive solute in spatially-periodic porous media were calculated theoretically [27,28] and numerically [29]. Other treatments of dispersion in porous media include surface and intraparticle transport [30,31] and dispersion in time-periodic flows [32].

This article is aimed at providing a coarse-scale description of the coupled transport of multi-component solutes in spatially periodic models of porous materials. In contrast with the single species transport, the phenomenological coefficients $\overline{\mathbf{U}}^*$, $\overline{\mathbf{D}}^*$ and $\overline{\mathsf{K}}^*$, governing concentrations $\overline{P}_i \quad (i = 1, \ldots, n)$ of a multi-component reactive solute are *square-matrix quantities* with generally nonzero coupling (off-diagonal) terms. The coarse-scale coupling, as embodied within these off-diagonal matrix elements is a macroscopic manifestation of the interstitial microscale coupling. The specific goal of this paper is calculation of the matrix coarse-scale transport coefficient describing transport of a multi-component solute for a given comparable data pertaining to the interstitial lengthscale.

Transport in systems of multiple reactive species was treated by the Generalized Taylor Dispersion (Macrotransport) Theory, for continuous species distributions [33]. Discrete sets of species were also studied [34] in application to flows in contactors and in general rectilinear pipe flows [35]. In application to transport in porous environment this problem has not yet been solved. In this paper we provide a general solution scheme for the calculation of matrix coarse-scale transport coefficients of a n-component reactive solute in a flow through a spatially-periodic model of a porous material. Specifically, we focus on the effect of microscale coupling on the macroscale transport properties. The solution scheme is illustrated by a calculation of these coefficients for the bundle-of-tube geometric model of a porous medium.

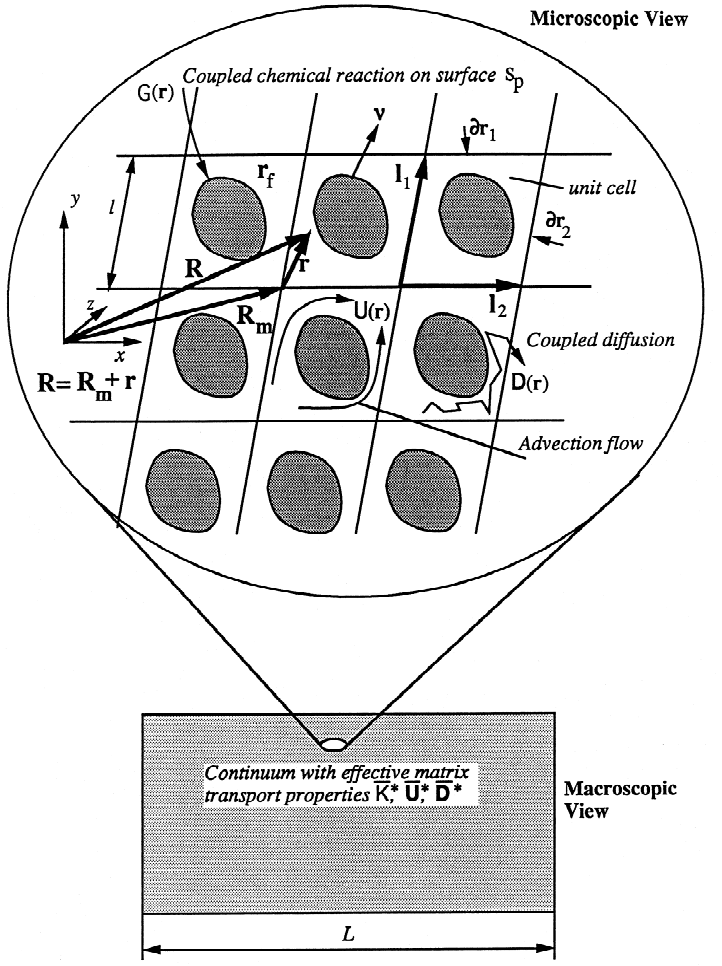

Figure 1. Convective-diffusive transport of a multicomponent solute in a spatially periodic model of a porous medium. Microscopic and macroscopic views. Microscale coupling is embodied in the diffusivity and reactivity matrices.

2. Mathematical model

Consider a dilute solution of n different kinds of particles/molecules flowing in a porous medium, which has a spatially periodic structure. This is characterized by a specified unit cell, which is indefinitely reproduced in a spatially-periodic manner in the effectively infinite space (Figure 1). The general position vector $\mathbf{R}$ may be decomposed as $\mathbf{R} = \mathbf{R_m}+\mathbf{r}$, where $\mathbf{r}$ is the continuous intracell position vector varying within the unit cell volume $\mathbf{r}_f$, and $\mathbf{R_m} = \mathbf{l}_i m_i$ is the discontinuous vector describing location of the unit cell within the effectively infinite lattice. Furthermore, $\mathbf{m} = \{m_1, m_2, m_3\}$ is a trio of integer numbers and $\mathbf{l}_i$, $i = 1, 2, 3$ are the basic lattice vectors. Component concentrations are organized in the column matrix $\mathsf{P}^{\backprime} = [P_1 P_2 ... P_n]^{\dagger}$ with $\dagger$ denoting the matrix-transposition operator. Alternatively, $\mathsf{P}^{\backprime} = \mathsf{P}^{\backprime}(\mathbf{R_m} - \mathbf{R_{m'}}, \mathbf{r}, t|\mathbf{r}')$ represents the column-matrix probability density of finding at a time t a n-component tracer particle in the vicinity of a point $(\mathbf{R_m}, \mathbf{r})$, given that at time $t = 0$ it was at $t = 0$ at the point $\mathbf{R}' = (\mathbf{R_{m'}}, \mathbf{r}')$.

The solute particles move within the solvent by advection, diffusion, and, possibly, external forces. On the bed-element surfaces the species undergo irreversible chemical reactions. These processes are described in terms of the square-matrix probability density P, defined by the relationship[1] $\mathsf{P}' = \mathsf{P}\mathtt{I}'$ with $\mathtt{I}' = [1...1]^\dagger$ one can write down the Fokker-Planck species transport equation in the form [26].

$$\frac{\partial \mathsf{P}}{\partial t} - \mathsf{L}\mathsf{P} = \delta(\mathbf{R} - \mathbf{R}')\delta(t)\mathtt{I}, \quad t > 0, \tag{3}$$

which is to be solved within the effectively infinite domain $\mathbf{r}_f\{\mathbf{m}\}$. In (3) $\mathtt{I}$ is the unit matrix, L is the matrix operator defined by

$$\mathsf{L} = -\nabla \cdot \mathbf{j}, \tag{4}$$

with $\nabla = \partial/\partial\mathbf{r}$, and the square-matrix species flux operator $\mathbf{j}$ given by the following constitutive equation:

$$\mathbf{j} = -\mathbf{D}(\mathbf{r}) \cdot \nabla + [\mathbf{U}(\mathbf{r}) + \mathbf{M}(\mathbf{r}) \cdot \mathbf{F}(\mathbf{r})]. \tag{5}$$

The matrix phenomenological coefficients appearing above are: $\mathbf{U}(\mathbf{r})$ – the advection velocity matrix, $\mathbf{D}(\mathbf{r}), \mathbf{M}(\mathbf{r})$ – the solute diffusivity and mobility matrices, related by the Stokes–Einstein equation $\mathbf{M} = \mathbf{D}/kT$ and $\mathbf{F}(\mathbf{r})$ is the external force matrix.

All elements of the matrices $\mathbf{D}, \mathbf{M}, \mathbf{U}, \mathbf{F}$ and G (see (6)) are assumed to depend on $\mathbf{r}$ only, i.e. to be spatially periodic functions. These matrix functions $\mathbf{D}(\mathbf{r}), \mathbf{M}(\mathbf{r})$, and, possibly, $\mathbf{U}(\mathbf{r}), \mathbf{F}(\mathbf{r})$ may have nonzero off-diagonal elements. This implies that transports of different solutes are coupled and cannot be considered independently, as described by Equations (3)–(5). These should be solved subject to the boundary conditions for P on the surface s_p of the bed elements:

$$\mathsf{S}\mathsf{P} \equiv [\boldsymbol{\nu}\mathbf{j} - \mathsf{G}(\mathbf{r})]\mathsf{P} = 0 \quad \text{on surface } s_p, \tag{6}$$

with $\boldsymbol{\nu}$ being the outer normal vector on the bed element surface (see Figure 1) and $\mathsf{G}(\mathbf{r})$ – the solute reactivity coefficient matrix. Additional boundary conditions are

$$\mathsf{P}, \mathbf{j}\mathsf{P} \text{ decay exponentially as } |\mathbf{R} - \mathbf{R}'| \to \infty, \tag{7a}$$

$$\mathsf{P}, \mathbf{j}\mathsf{P} \text{ are continuous across superficial unit cell faces } \partial\mathbf{r}_k (k = 1, 2, 3). \tag{7b}$$

The problem (3)–(7) is solved by a variant of the method of statistical moments [26, 27], extended here to include coupled transport of multicomponent reactive species. We will be concerned with temporal behavior of the local and total square-matrix polyadic moments, of orders $k = 0, 1, 2, \ldots$, respectively, defined by

$$\mathbf{P}_k(\mathbf{r}, t|\mathbf{r}') = \sum_{\mathbf{m}} (\mathbf{R}_{\mathbf{m}} - \mathbf{R}_{\mathbf{m}'})^k \mathsf{P}(\mathbf{R}_{\mathbf{m}} - \mathbf{R}_{\mathbf{m}'}, \mathbf{r}, t|\mathbf{r}), \tag{8a}$$

[1] Bold letters denote tensor and vector quantities. Capital "Geneva" font letters ($\mathsf{P}, \mathbf{D}, \mathbf{U}$, etc.) will be reserved for square matrix quantities and operators (composed from scalar, vector or tensor elements). Column and row matrices will be marked by "Geneva" letters with reverse prime superscript ' ($\mathsf{P}', \mathsf{W}', \mathsf{A}'$). "Times" font letters (P, T, t, etc.) will denote nonmatrix quantities. The symmetrization operator $(...)^s$ is meant to act on dyadics, which may serve as matrix elements, but not on the matrices themselves. When the transposition operator $(...)^\dagger$ is applied to matrices composed of dyadic elements, the dyadics remain unchanged.

$$\mathbf{M}_k(t|\mathbf{r}') = \overline{\mathbf{P}}_k(\mathbf{r}, t|\mathbf{r}'), \tag{8b}$$

where for any **r**-dependent matrix function, for example, species-concentration matrix P, the overbar operation is defined by an integration over the unit cell volume $\mathbf{r}_f$:

$$\overline{\mathsf{P}} = \int_{\mathbf{r}_f} \mathsf{P}(\ldots, \mathbf{r}, \ldots)\, \mathrm{d}\mathbf{r}. \tag{9}$$

This expression provides a definition of the coarse-scale species concentration.

Each of the local moments $\mathbf{P}_m (m = 0, 1, 2, \ldots)$ satisfies the following system of equations and boundary conditions

$$\frac{\partial \mathbf{P}_m}{\partial t} - \mathsf{L}\mathbf{P}_m = \delta_{m0}\delta(\mathbf{r} - \mathbf{r}')\delta(t)\mathtt{I} \quad \mathbf{r} \in \mathbf{r}_f, \quad \mathsf{S}\mathbf{P}_m = 0 \quad \mathbf{r} \in s_p, \quad t > 0, \tag{10a,b}$$

obtainable from (3) with the help of definition (8a). Additionally, with use of (8b), $\mathbf{P}_m$ may be shown to obey the so-called "jump" conditions, imposed on the opposite unit-cell faces:

$$[|\mathsf{P}_0|] = 0, \quad [|\nabla \mathsf{P}_0|] = 0; \tag{11a}$$

$$[|\mathbf{P}_1|] = -[|\mathbf{r}\mathsf{P}_0|], \quad [|\nabla \mathbf{P}_1|] = -[|\nabla(\mathbf{r}\mathsf{P}_0)|]; \tag{11b}$$

$$[|\mathbf{P}_2|] = [|\mathbf{P}_1\mathsf{P}_0^{-1}\mathbf{P}_1|], \quad [|\nabla \mathbf{P}_2|] = [|\nabla(\mathbf{P}_1\mathsf{P}_0^{-1}\mathbf{P}_1)|]. \tag{11c}$$

In the above $[|...|]$ denotes the "jump" of any polyadic-valued matrix function between the equivalent points lying on the opposite faces $\partial\mathbf{r}_k$ of the unit cell.

3. Solution for the local zero-order moment

The problem posed for the zero-order moment by Equations (10a,b) with $m = 0$, (11a) may be treated by the method of separation of variables in its matrix form. Accordingly, we construct the solution for this problem in the form of an eigenfunction expansion

$$\mathsf{P}_0(\mathbf{r}, t|\mathbf{r}') = \sum_{k=1}^{\infty} \mathsf{W}_k^{\backprime}(\mathbf{r}) \otimes \mathsf{A}_k^{\backprime}(\mathbf{r}') \exp(-\lambda_k t), \tag{12}$$

where $\otimes$ denotes the tensor, or right-Kronecker matrix product [36] and the column- and row-matrix functions $\mathsf{W}_k^{\backprime}$ and $\mathsf{A}_k^{\backprime} (k = 1, 2, ...)$ are the respective solutions of the basic unit-cell-matrix eigenvalue problems (A1), (A2). Some properties of these eigensolutions are summarized in Appendix A. In fact, expansion (12) is valid, when each set of eigenfunctions $\{\mathsf{W}_k^{\backprime}\}, \{\mathsf{A}_k^{\backprime}\}$ is complete in the functional space $\mathsf{L}_2(\mathbf{r}_f)$, associated with the interstitial volume $\mathbf{r}_f$. Existence of the completeness property cannot be taken for granted, albeit in many cases pertaining to convective-diffusive transport processes this property can be proven [37–39].

Existence of solution for the zero-order local moment in the form (12) is a fundamental assumption, underlying the subsequent analyses. Solution (12) may be further used to obtain both short- and long-time behaviors of the higher-order local moments, as well as their spatial distributions. The general route of constructing such solutions [40] is based on the fundamental property of P_0, according to which it serves as the Green's function for the solutions for the higher-order moments $\mathbf{P}_k (k = 1, 2, ...)$.

We will further be interested in the asymptotic long-time forms of $\mathbf{P}_k$. For P_0 such a form may be obtained by an appropriate truncation of the series in the right-hand side of (12). The

minimum number of terms to be retained is dictated by the structure of the eigensolutions of the EVPs (A1), (A2). In this respect, without loss of generality, we will assume that all n elements of each pair of eigensolutions $\mathsf{W}_k^{\backprime}$, $\mathsf{A}_k^{\backprime}$ are *linearly independent*, i.e., transports of all n solutes are strongly coupled at the interstitial scale.

Consider the following long-time approximations of the zero-order local moment:

(i) One term asymptotic approximation, which means that all terms with $k > 1$ in the right-hand side of (12) are neglected, as exponentially small, compared to the leading-order term:

$$\mathsf{P}_0(\mathbf{r}, t|\mathbf{r}') = \mathsf{W}_1^{\backprime}(\mathbf{r}) \otimes \mathsf{A}_1^{\backprime}(\mathbf{r}') \exp(-\lambda_1 t)(1 + \text{exp}), \tag{13}$$

where 'exp' denotes exponentially small terms. This is valid for sufficiently long times, explicitly, for $t \gg t_1 = [\text{Re}(\lambda_2) - \text{Re}(\lambda_1)]^{-1}$, where λ_2 is the eigenvalue with the second largest real part immediately following λ_1.

(ii) n-term asymptotic, where the series in (12) are truncated after n terms, with the result expressible in the square-matrix notation (see Appendix A)

$$\mathsf{P}_0(\mathbf{r}, t|\mathbf{r}') = \mathsf{W}_1(\mathbf{r}) \exp(-\Lambda_1 t)\mathsf{A}_1(\mathbf{r}')(1 + \text{exp}). \tag{14}$$

In the above $\mathsf{W}_1, \mathsf{A}_1, \Lambda_1$ are square matrices composed of n leading subsequent eigensolutions. Approximation (14) is valid for $t \gg t_n = [\text{Re}(\lambda_{n+1}) - \text{Re}(\lambda_n)]^{-1}$, which is generally less than t_1, since normally the distances between the (real parts of) subsequent eigenvalues increase with increasing n.

The objective of the solution is to provide a scheme for the calculation of the coarse-scale solute concentrations represented by matrix $\overline{\mathsf{P}}$ (see (9)). We will be interested in circumstances where $\overline{\mathsf{P}}$ is governed by the corresponding coarse-scale transport equation (cf. Equation (1))

$$\frac{\partial \overline{\mathsf{P}}}{\partial t} + \overline{\mathbf{U}}^* \cdot \overline{\nabla \mathsf{P}} - \overline{\mathbf{D}}^* : \overline{\nabla \nabla \mathsf{P}} + \overline{\mathsf{K}}^* \overline{\mathsf{P}} = \mathsf{V}(\mathbf{r}')\delta(\overline{\mathbf{R}} - \overline{\mathbf{R}}')\delta(t), \tag{15}$$

wherein $\overline{\nabla} = \partial/\partial\overline{\mathbf{R}}$ and $\overline{\mathbf{R}}$ is the coarse-scale position vector, i.e. the continuous analog of the discontinuous position vector $\mathbf{R_m}$. *Matrix* transport coefficients appearing in this equation are: coarse-scale reactivity $\overline{\mathsf{K}}^*$, velocity vector $\overline{\mathbf{U}}^*$, and dispersivity dyadic $\overline{\mathbf{D}}^*$. The matrix function $\mathsf{V}(\mathbf{r}')$ accounts for dependence of $\overline{\mathsf{P}}$ upon the initial tracer position within the unit cell. It is used for formulating initial conditions, imposed on $\overline{\mathsf{P}}$ [27]. These coefficients are to be determined by matching the total moments

$$\overline{\mathbf{M}}_k(t|\mathbf{r}') = \int_{\overline{\mathbf{R}}_\infty} (\overline{\mathbf{R}} - \overline{\mathbf{R}}')^k \overline{\mathsf{P}}(\overline{\mathbf{R}} - \overline{\mathbf{R}}', t|\mathbf{r}')\, \mathrm{d}^3\overline{\mathbf{R}}, \quad (k = 0, 1, 2, \ldots) \tag{16}$$

of the concentration matrix $\overline{\mathsf{P}}$, governed by Equation (15), with their exact long-time moments $\mathbf{M}_k$ defined by (8b), which will be calculated from the solution of problems (10)–(11).

In the following we will calculate these long-time moments and, on that basis, the coarse-scale transport coefficients via the n-term asymptotic solution scheme. A comparable one-term asymptotic solution will be further deduced as a particular case of the n-term asymptotic solution.

4. The n-term asymptotic solution

Starting with the asymptotic formula (14), we will develop solutions for the first and second-order moments under the assumption that the eigenvalues composing the leading-order eigen-

solution matrix Λ_1 are all different. A situation when this requirement does not hold is described in section 6. The solution for the first-order local moment is constructed in the form

$$\mathbf{P}_1(\mathbf{r}, t|\mathbf{r}') \cong \{[\mathsf{W}_1\mathbf{Q}t + \mathbf{B}(\mathbf{r})]\exp(-\Lambda_1 t)\mathsf{A}_1(\mathbf{r}') + \mathsf{W}_1\exp(-\Lambda_1 t)\mathbf{E}_1(\mathbf{r}')\}(1+\exp), \quad (17)$$

where $\mathbf{Q}$ is a constant vector-valued *diagonal* matrix, $\mathbf{B}(\mathbf{r})$ is a vector-valued intracell matrix field, both to be determined, and $\mathbf{E}_1$ any $\mathbf{r}'$-dependent, vector-valued square matrix. The quantities $\mathbf{Q}$ and $\mathbf{B}(\mathbf{r})$ are determined by introduction of the trial solution (17) in the problem (10)–(11b), which eventually leads to (see Appendix B)

$$\mathbf{Q} = \mathrm{Diag}\int_{\partial\mathbf{r}_0} \mathrm{d}^2\mathbf{s}\cdot(\mathsf{A}_1\mathbf{j}\mathsf{W}_1 + \nabla\mathsf{A}_1\cdot\mathbf{D}\mathsf{W}_1)\mathbf{r}. \quad (18)$$

The intracell problem governing the $\mathbf{B}$-field and its properties are specified in Appendix B.

The trial solution for the second-order local moment $\mathbf{P}_2$ is:

$$\mathbf{P}_2(\mathbf{r}, t|\mathbf{r}') \cong \{[\mathsf{W}_1(\mathbf{Q}^2t^2+2t\boldsymbol{\Delta})+2t\mathbf{B}(\mathbf{r})\mathbf{Q}+\mathbf{H}(\mathbf{r})]^s\exp(-\Lambda_1 t)\mathsf{A}_1(\mathbf{r}')+\cdots\}(1+\exp), \quad (19)$$

where $\mathbf{H}(\mathbf{r})$ is a square-matrix dyadic-valued field, $\boldsymbol{\Delta}$ is a constant *diagonal* dyadic-valued matrix. The mathematical procedure for the determination of $\mathbf{H}(\mathbf{r})$ and $\boldsymbol{\Delta}$ is similar to the one used in the solution for the first moment (see Appendix B), and eventually yields the following value of $\boldsymbol{\Delta}$:

$$\boldsymbol{\Delta} = \mathrm{Diag}\,\wp(\mathbf{B}\mathsf{W}_1^{-1}\mathbf{B}) - \mathrm{Diag}[\langle\mathsf{A}_1, \mathbf{B}\rangle\mathbf{Q}]^s, \quad (20)$$

where, generically, for any matrix function $\mathbf{E}$, the operator $\wp$ is defined by

$$\wp(\mathbf{E}) = -\frac{1}{2}\int_{\partial\mathbf{r}_0} \mathrm{d}^2\mathbf{s}\cdot(\mathsf{A}_1\mathbf{j}\mathbf{E} + \nabla\mathsf{A}_1\cdot\mathbf{D}\mathbf{E}). \quad (21)$$

The angular brackets in (20) mean inner product defined in (A4).

5. Coarse-scale transport coefficients

The expressions for the total matrix moments are obtained by integration of Equations (14), (17) and (19) over the unit-cell volume, which yields

$$\mathsf{M}_0 \cong \overline{\mathsf{W}}_1\exp(-\Lambda_1 t)\mathsf{A}_1(\mathbf{r}')(1+\exp), \quad (22a)$$

$$\mathbf{M}_1 \cong \{[\overline{\mathsf{W}}_1\mathbf{Q}t + \overline{\mathbf{B}}]\exp(-\Lambda_1 t)\mathsf{A}_1(\mathbf{r}')+\cdots\}(1+\exp), \quad (22b)$$

$$\mathbf{M}_2 \cong \{\overline{\mathsf{W}}_1[\mathbf{Q}^2t^2 + 2t\boldsymbol{\Delta}] + 2t\overline{\mathbf{B}}\mathbf{Q} + \overline{\mathbf{H}} + \cdots\}^s\exp(-\Lambda_1 t)\mathsf{A}_1(\mathbf{r}')(1+\exp), \quad (22c)$$

wherein the terms irrelevant for the determination of the matrix transport coefficients are omitted.

We will match the above exact long-time moments with their counterparts $\overline{\mathbf{M}}_k$ (see (8b)), governed by the model equation (15). Equations for $\overline{\mathbf{M}}_k$ may be obtained by multiplication of both sides of (15) by $(\overline{R} - \overline{R}')^m, m = 0, 1, 2$, integration over infinite space with the attenuation condition (7a). Solution of these equations and moment matching ultimately yield

$$\overline{\mathsf{K}}^* = \overline{\mathsf{W}}_1\Lambda_1\overline{\mathsf{W}}_1^{-1}, \quad (23a)$$

$$\overline{\mathsf{U}}^* = \overline{\mathsf{W}}_1 \mathbf{Q} \overline{\mathsf{W}}_1^{-1} + (\overline{\mathsf{K}}^* \overline{\mathbf{B}} - \overline{\mathbf{B}} \Lambda_1) \overline{\mathsf{W}}_1^{-1}, \tag{23b}$$

$$\overline{\mathbf{D}}^* = \overline{\mathsf{W}}_1 \boldsymbol{\Delta} \overline{\mathsf{W}}_1^{-1} + (\overline{\mathbf{B}} \mathbf{Q} - \overline{\mathbf{U}}^* \overline{\mathbf{B}})^s \overline{\mathsf{W}}_1^{-1} + \frac{1}{2} (\overline{\mathsf{K}}^* \overline{\mathbf{H}} - \overline{\mathbf{H}} \Lambda_1) \overline{\mathsf{W}}_1^{-1}, \tag{23c}$$

and also $\mathsf{V} = \mathsf{A}_1$.

We may repeat this solution scheme, using the one-term approximation (13) for the zero-order local moment. As a result, we obtain *nonmatrix* expressions for the coarse-scale reactivity, velocity and dispersivity, respectively, equal to the leading elements $\lambda_1, \mathbf{Q}_{11}$ and $\boldsymbol{\Delta}_{11}$ of the corresponding matrices $\Lambda_1, \mathbf{Q}$ and $\boldsymbol{\Delta}$. These coefficients appear in the equation (cf. (15)).

$$\frac{\partial \overline{\mathsf{P}}^{(1)}}{\partial t} + Q_{11} \cdot \overline{\nabla \mathsf{P}}^{(1)} - \boldsymbol{\Delta}_{11} : \overline{\nabla \nabla \mathsf{P}}^{(1)} + \lambda_1 \overline{\mathsf{P}}^{(1)} = V(\mathbf{r}') \delta(\overline{\mathbf{R}} - \overline{\mathbf{R}}') \delta(t), \tag{24}$$

governing the coarse-scale solute concentration matrix $\overline{\mathsf{P}}$ for $t \to \infty$. Explicitly, for $t \gg t_n = [\mathrm{Re}(\lambda_{n+1}) - \mathrm{Re}(\lambda_n)]^{-1}$, the coarse-scale coupling becomes ineffective and the system evolution may be determined from Equation (24).

We will finally note that the constant matrix $\overline{\mathsf{W}}_1$ appearing in (23), may be interpreted as a species-partition matrix. Specifically, it characterizes the distribution of matter between the different components prevailing at the coarse scale.

6. Particular cases

6.1. Nonreactive species

In the absence of reactions ($\mathsf{G}(\mathbf{r}) = 0$) one can show (see Appendix A) that the total species' mass is conserved. On the coarse scale matter is equally distributed between the species, i.e., the solute partition matrix $\overline{\mathsf{W}}_1$ is the unity matrix, even in the presence of the interstitial coupling, embodied in $\mathsf{W}_1(\mathbf{r})$. One can also see from (A14c) that the species that are inert at the microscale are also nonreactive at the coarse scale.

No one-term asymptotic solution exists in this case. The n-term asymptotic solution constructed in sections 4, 5 is also invalid, since in the present case the diagonal matrix Λ_1 consists of identical eigenvalues. A generalization of the n-term asymptotic solution method developed in this case yields the following expressions for the transport coefficients of nonreactive species

$$\overline{\mathsf{K}}^* = 0, \tag{25a}$$

$$\overline{\mathbf{U}}^* = \int_{\partial \mathbf{r}_0} \mathrm{d}^2 \mathbf{s} \cdot \mathbf{j} \mathsf{W}_1 \mathbf{r}, \tag{25b}$$

$$\overline{\mathbf{D}}^* = -\frac{1}{2} \int_{\partial \mathbf{r}_0} \mathrm{d}^2 \mathbf{s} \cdot \mathbf{j} (\mathbf{B} \mathsf{W}_1^{-1} \mathbf{B}) - (\mathbf{Q} \overline{\mathbf{B}})^s, \tag{25c}$$

together with $\mathsf{V} = \mathtt{I}$. The solution of the dyadic-valued $\mathbf{H}$-field is not required for the calculation of $\overline{\mathbf{D}}^*$, because $\Lambda_1 = 0$.

In general, the velocity matrix $\overline{\mathbf{U}}^*$, given by (25b) is not diagonal, even if the microscale velocity matrix $\mathbf{U}(\mathbf{r})$ is a spherical matrix, i.e. $\mathbf{U}(\mathbf{r}) = \mathrm{U}(\mathbf{r})\mathtt{I}$. The coupling embodied in $\overline{\mathbf{U}}^*$ stems from the fact that $\mathsf{W}_1(\mathbf{r})$ may generally have nonzero off-diagonal terms (vanishing upon

integration over $\mathbf{r}_f$), which contribute to the off-diagonal species-flux members, nonvanishing upon interstitial averaging. In the case of pure diffusion, where the microscale advection velocity and external forces are absent ($\mathbf{U}(\mathbf{r}) = \mathbf{0}, \mathsf{F}(\mathbf{r}) = \mathbf{0}$), we can show that $\mathsf{W}_1(\mathbf{r}) = \mathtt{I}$, which yields $\overline{\mathbf{U}}^* = \mathbf{0}$, i.e. all species have zero coarse-scale velocity.

6.2. Removable microscale coupling

This important case concerns the situation where the problem (3)–(7) may be rewritten in terms of certain linear combinations, say, $P_i^o \ \ (i = 1, 2, \ldots, n)$, of the species concentrations P_i, in such a way that the coupling at the interstitial scale is removed. Examples of such cases are:

$$\text{(i) } \mathsf{G}(\mathbf{r}) = G(\mathbf{r})\mathtt{I}, \quad \mathbf{D}(\mathbf{r}) = \mathsf{D}\mathbf{I} = \text{const}, \quad \mathbf{U}(\mathbf{r}) = \mathbf{U}(\mathbf{r})\mathtt{I}, \quad \mathbf{F}(\mathbf{r}) = \mathbf{F}(\mathbf{r})\mathtt{I}, \tag{26a}$$

$$\text{(ii) } \mathsf{G}(\mathbf{r}) = \mathsf{G} = \text{const}, \quad \mathbf{D}(\mathbf{r}) = D(\mathbf{r})\mathtt{I}, \quad \mathbf{U}(\mathbf{r}) = \mathbf{U}(\mathbf{r})\mathtt{I}, \quad \mathbf{F}(\mathbf{r}) = \mathbf{F}(\mathbf{r})\mathtt{I}, \tag{26b}$$

wherein, $G(\mathbf{r}), D, \mathbf{U}(\mathbf{r}), \mathbf{F}(\mathbf{r})$ are nonmatrix quantities, and $\mathbf{I}$ is a (nonmatrix) unit tensor. Referring, for example, to case (26a), we may notice that, if matrix D is simple, it may be transformed into the diagonal form by means of the transformation

$$\mathsf{D}^o = \mathfrak{R}\mathsf{D} \equiv \mathsf{T}^{-1}\mathsf{D}\mathsf{T}, \tag{27a}$$

where D^o is the diagonal matrix composed from the eigenvalues of D, and T is a nonsingular constant transition matrix. Normally, D is a positive-definite symmetric (Hermitian) matrix. Therefore, it has n real eigenvalues and corresponding real eigenvectors, which may be used to compose the transformation matrix T at least in circumstances where all the eigenvalues of D are different.

We may further introduce new solute concentrations $\mathsf{P}^o = \mathfrak{R}\mathsf{P} = \mathsf{T}^{-1}\mathsf{P}\mathsf{T}$, in terms of which the microscale species-transport processes are clearly uncoupled. The coarse-scale transport coefficients governing transport of the transformed solute concentration matrix $\overline{\mathsf{P}}^o$ (averaged over $\mathbf{r}_f$) may be calculated independently for each constituent [27]. We will call these concentrations and the corresponding macroscopic transport coefficients $\overline{\mathsf{K}}^o, \overline{\mathbf{U}}^o, \overline{\mathbf{D}}^o$ *canonic* solute concentrations and coefficients. The transport coefficients governing the original concentration $\overline{\mathsf{P}}$ may be calculated by the inverse transformation, namely,

$$\overline{\mathsf{K}}^* = \mathfrak{R}^{-1}\overline{\mathsf{K}}^o = \mathsf{T}\overline{\mathsf{K}}^o\mathsf{T}^{-1}, \text{ etc}, \tag{27b}$$

in order to obtain the comparable transport properties governing $\overline{\mathsf{P}}$ (see section 7).

6.3. Diffusion and reaction in the absence of convection

This is the case, where convection is absent at the microscale. In this case the basic eigenvalue problems simplify (see Appendix A) and we obtain from (18) that $\mathbf{Q} = \mathbf{0}$. As a result, the coarse-scale velocity (23b) reduces to the following traceless matrix

$$\overline{\mathbf{U}}^* = (\overline{\mathsf{K}}^*\overline{\mathbf{B}} - \overline{\mathbf{B}}\Lambda_1)\overline{\mathsf{W}}_1^{-1}. \tag{28}$$

Employing $\overline{\mathsf{W}}_1$ as a transition matrix, we may show that $\overline{\mathbf{U}}^*$ given above is equivalent to a matrix $\overline{\mathbf{U}}^*_W$, in which diagonal elements vanish and only off-diagonal terms may differ

from zero. This basically differs from comparable results that were obtained for transport of multiple species in tube and channel flows [41], in which case *all* elements of $\overline{\mathsf{U}}^*$ vanish in the absence of microscale advection. However, the effect of off-diagonal terms in $\overline{\mathsf{U}}^*_W$ on $\overline{\mathsf{P}}$ diminishes with time, and for $t \gg t_n$ the species transport becomes uncoupled (see section 5).

6.4. TRANSPORT IN TERMS OF THE TOTAL SOLUTE CONCENTRATION

In some situations we may be interested in a total solute-mass concentration by summing up the concentrations of all components

$$\overline{\mathsf{P}}^t = \sum_{i=1}^{n} \overline{\mathsf{P}}_i = \mathtt{I}^{\backprime\dagger} \overline{\mathsf{P}} \mathtt{I}^{\backprime}. \tag{29}$$

The equation governing transport and evolution of $\overline{P}^t$ may be obtained by a multiplication of both sides of the coarse-scale equation (24) by the column matrix $\mathtt{I}^{\backprime}$ from the right, and by the row matrix $\mathtt{I}^{\backprime\dagger}$ from the left, to obtain the following equation for $\overline{P}^t$:

$$\frac{\partial \overline{P}^t}{\partial t} + \mathbf{Q}_{11} \cdot \overline{\nabla P}^t - \mathbf{\Delta}_{11} : \overline{\nabla\nabla P}^t + \lambda_i \overline{P}^t = V^t(\mathbf{r}')\delta(\overline{\mathbf{R}} - \overline{\mathbf{R}}')\delta(t), \tag{30}$$

wherein the scalar function $V^t(\mathbf{r}') = \mathtt{I}^{\backprime\dagger} \mathsf{V}(\mathbf{r}') \mathtt{I}^{\backprime}$.

One thus finds that the nonmatrix coarse-scale transport properties, derived in the course of one-term asymptotic solution, govern also the total solute concentration $\overline{\mathsf{P}}^t$. This concentration may be interpreted as a probability of finding a single scalar tracer particle in any of the species, without distinguishing between them. We will finally note that Equation (30) is valid for asymptotically long times $t \gg t_1 = [\mathrm{Re}(\lambda_2) - \mathrm{Re}(\lambda_1)]^{-1}$, for which the validity of the one-term approximation (12) has been established. Validity of Equation (30) does not extend to earlier times, i.e., to those when approximation (14) and the corresponding n-term asymptotic solution hold.

7. Example: Coupled dispersion in a bundle of tubes

The mathematical solutions obtained in the previous sections enable the calculation of coarse-scale matrix-transport coefficients for any unit-cell geometry, characterizing the interstitial structure of a given material. For real materials such calculations, even for one species, constitute a significant computational task [42]. In this section we will illustrate the general theory developed above on the example of the bundle-of-tubes model of a porous medium. Solution for such a simplified geometry helps to rationalize the effects of the various microscale parameters and transport properties on coarse-scale coefficients. On the other hand, such a solution can serve as a test of computational codes to be developed for more general interstitial geometries.

Consider convective-diffusive transport of two species of concentrations $\mathsf{P}^{\backprime} = [P_1 P_2]^\dagger$ moving in long circular capillary tubes of radius a (Figure 2). Equation (3), governing the corresponding square matrix solute concentration P in each tube, takes the following form

$$\frac{\partial \mathsf{P}}{\partial t} + U(r)\frac{\partial \mathsf{P}}{\partial x} = \mathsf{D}\left[\frac{1}{r}\frac{\partial}{\partial r}\left(r\frac{\partial \mathsf{P}}{\partial r}\right) + \frac{\partial^2 \mathsf{P}}{\partial x^2}\right], \qquad 0 < r < a, \quad -\infty < x < \infty. \tag{31}$$

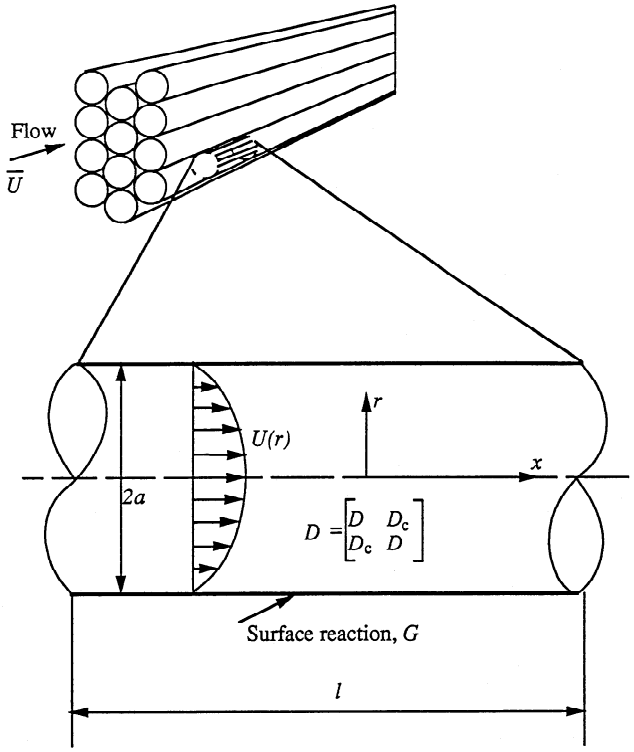

Figure 2. Coupled convective-diffusive transport of a two-component inert solute in a flow in a bundle of tube model of a porous medium.

In the above $U(r) = 2\overline{U}(1 - r^2/a^2)$ is the solute-flow velocity profile, with $\overline{U}$ being the average flow velocity, and D a constant solute diffusivity matrix

$$\mathsf{D} = \begin{bmatrix} D & D_c \\ D_c & D \end{bmatrix},$$

possessing all positive elements, with $D_c < D$.

The boundary conditions for P are (cf. (6)):

$$\mathsf{D}\frac{\partial \mathsf{P}}{\partial r} = G\mathsf{P} \quad \text{at} \quad r = a, \tag{32}$$

and the attenuation conditions at $x \to \pm\infty$. In the above it is assumed that the species undergo a first-order irreversible surface reaction on the wall with the same constant coefficient G.

We can formulate the microscale problem, as posed above, using a periodic unit cell, the length l of which is arbitrary (see Figure 2). In these circumstances, one can identify r as the microscale bounded variable, while x serves as an unbounded coarse-scale coordinate $\overline{\mathbf{R}}$.

The matrix D has eigenvalues $\delta_1 = D + D_c, \delta_2 = D - D_c$. These quantities, respectively, represent the diffusivities of the "fast" and the "slow" canonic solute components $(\delta_2 < \delta_1)$. We will use the corresponding eigenvectors of the matrix D to form the transition matrix T

$$\mathsf{T} = \begin{bmatrix} 1 & -1 \\ 1 & 1 \end{bmatrix}.$$

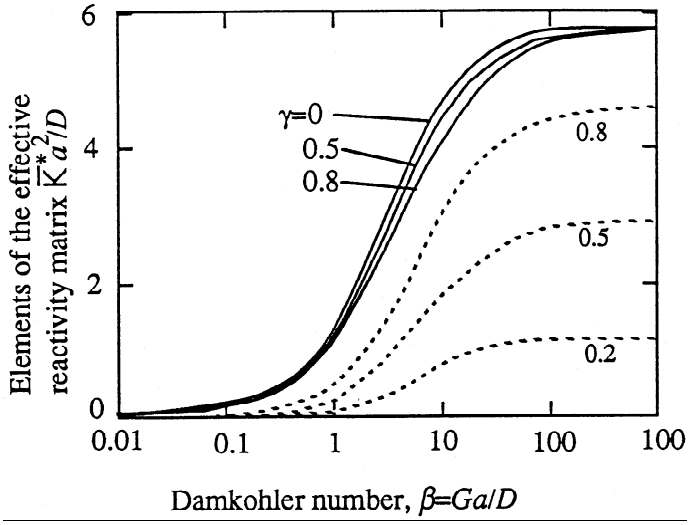

Figure 3. Elements of the effective reactivity matrix, normalized by D/a^2. The curve plotted for $\gamma = D_c/D = 0$ corresponds to uncoupled constituents. Solid lines: $\overline{K}^*_{11}, \overline{K}^*_{22}$, dotted lines: $\overline{K}^*_{12}, \overline{K}^*_{21}$.

We use this in the transformations $\mathsf{P}^o = \mathfrak{R}\mathsf{P}, \mathsf{D}^o = \mathfrak{R}\mathsf{D}$ (see (27a)), allowing to rewrite the problem (31)–(32) in terms of the canonic solute concentration matrix P^o in an uncoupled form. Namely, P^o satisfies Equations (31), (32) wherein D is replaced by $\mathsf{D}^o = \mathrm{Diag}[\delta_1, \delta_2]$. The long-time coarse-scale (axial) transport coefficients $\overline{K}^o_i, \overline{U}^o_i, \overline{D}^o_i (i = 1, 2)$ for each canonic component may be determined independently in the form:

$$\overline{K}^o_i = f_K(\beta_i)\,\frac{\delta_i}{a^2}, \quad \overline{U}^o_i = f_U(\beta_i)\overline{U}, \quad \overline{D}^o_i = f_D(\beta_i)\,\frac{\overline{U}a^2}{48\delta_i} + \delta_i, \quad i = 1, 2, \qquad \text{(33a,b,c)}$$

and the functions f_K, f_U, and f_D depend on the dimensionless Damkohler numbers $\beta_i = Ga/\delta_i, i = 1, 2$ of the canonic components.

The functions f_K, f_U, and f_D were calculated by Sankarasubramanian and Gill [7]. We will use their results to calculate the matrix transport coefficients governing $\overline{\mathsf{P}}$ by applying the inverse transformation (27), namely $\overline{\mathsf{K}}^* = \mathfrak{R}^{-1}\overline{\mathsf{K}}^o$, $\overline{\mathsf{U}}^* = \mathfrak{R}^{-1}\overline{\mathsf{U}}^o$, $\overline{\mathsf{D}}^* = \mathfrak{R}^{-1}\overline{\mathsf{U}}^o$, where $\overline{\mathsf{K}}^o, \overline{\mathsf{U}}^o, \overline{\mathsf{D}}^o$ are diagonal matrices formed by the corresponding members of (33a–c).

8. Results

Figure 3 presents the elements of the effective axial reactivity matrix $\overline{\mathsf{K}}^*$. The curve calculated for $\gamma = D_c/D = 0$ corresponds to uncoupled constituents, for which $\overline{K}^*_{12} = \overline{K}^*_{21} = 0$. In this case the diagonal elements $\overline{K}^*_{11} = \overline{K}^*_{22}$ of the reactivity matrix monotonically increase from zero at $\beta = 0$, to $5.784D/a^2$ at $\beta \to \infty$. A similar trend prevails also with coupling (for $\gamma > 0$), although K_{11} and K_{12} slightly decrease with increasing γ. This results from solute mass redistribution in favor of coupling elements. That is, the coarse-scale reaction rate of each (say, first) component is governed, not only by P_1 (as in the absence of coupling), but also by the coupling component concentration P_2. The relative strength of each of these two reaction rates is controlled (for long times) by the cross-sectional mass partition between the components, as embodied within the partition matrix $\overline{\mathsf{W}}_1$.

Another effect of coupling is to create non-zero off-diagonal reactivity elements $\overline{K}^*_{12} = \overline{K}^*_{21} > 0$ which increase with increasing γ. In the limit $\beta \to \infty, \overline{K}^*_{12}$ and $\overline{K}^*_{21} = 0$ reach

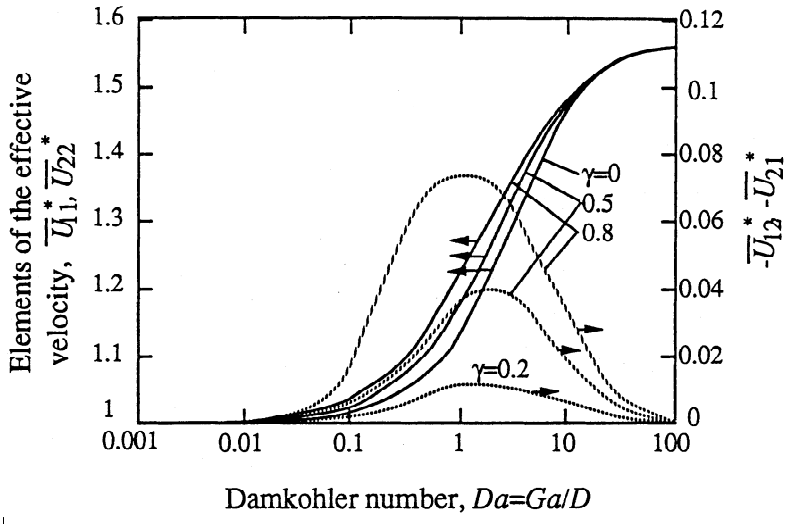

Figure 4. Elements of the effective velocity matrix, normalized by the mean solvent velocity $\overline{U}$. The curve plotted for $\gamma = D_c/D = 0$ corresponds to uncoupled constituents. Solid lines: $\overline{U}_{11}^*, \overline{U}_{22}^*$, dotted lines: $-\overline{U}_{12}^*, -\overline{U}_{21}^*$.

their (γ-dependent) asymptotic values. The long-time reaction rate for each component is governed by $\exp[-(\overline{K}_{11}^* + \overline{K}_{12}^*)t]$, decreases with increasing $\gamma = D_c/D$ (see Figure 3). We may rationalize this by noting that an increase of the coupling parameter γ is tantamount to an increase of the coupling molecular diffusivity D_c (with D fixed) which helps the species to reach the reactive surface and, thus, promotes the reaction rate.

Figure 4 presents the elements of the effective axial solute velocity. In the absence of coupling($\gamma = 0$) the effect of the solute reactivity, as expressed via the Damkohler number β, is to increase the axial solute velocity. This results from the solute depletion (caused by reaction) from the region near the wall and the concomitant solute concentration redistribution in favor of the central region, where the flow velocity is larger. This effect is most profound for large Damkohler numbers (diffusion-controlled reaction), where both of these velocities reach $1.56\overline{U}$.

The effect of the microscale-coupling parameter γ is (i) to decrease the diagonal elements $\overline{U}_{11}^* = \overline{U}_{22}^*$ of the solute velocity matrix and (ii) to give rise to *negative* off-diagonal terms $\overline{U}_{12}^* = \overline{U}_{21}^*$. Therefore, the total convective solute flux for each component, e.g. given for the first component by $\overline{U}_{11}^*\overline{P}_1 + \overline{U}_{12}^*\overline{P}_2$, decreases. We may explain this by noting that the effect of increasing coupling reactivity D_c (i.e., increasing γ) is to bring about a more uniform cross-sectional solute distribution, which is macroscopically manifested by a decrease of the total convective flux (see Equation (2)). The off-diagonal matrix velocity elements result from the difference between the average speeds $\overline{U}_{11}^0, \overline{U}_{22}^0$ of the canonic components, which are controlled by the respective canonic reactivity parameters $\beta_1 = Ga/(D + D_c), \beta_2 = Ga/(D - D_c)$. The speeds $\overline{U}_{11}^0, \overline{U}_{22}^0$ are equal at the limiting situations of small β (where they are equal to the solvent velocity $\overline{U}$), and for large β (where they are both equal to $1.56\overline{U}$). In the range of intermediate values of β a shift between β_1 and β_2 results in nonequal elements $\overline{U}_{11}^0 \neq \overline{U}_{22}^0$ with the difference increasing with growing γ. In particular, when D_c is close to D, the fastest canonic component behaves as a neutral species, while the slowest one exhibits a strongly reactive behavior. In this situation the difference between $\overline{U}_{11}^0$ and $\overline{U}_{22}^0$ reaches the

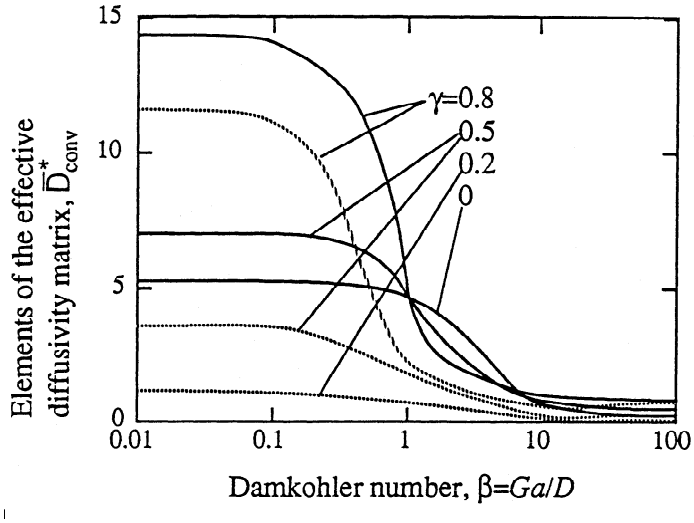

Figure 5. Elements of the convective part of the effective diffusivity matrix, normalized by $\overline{U}^2 a^2/48D$. The curve plotted for $\gamma = D_c/D = 0$ corresponds to uncoupled constituents. Solid lines: $\overline{D}^*_{11}, \overline{D}^*_{22}$, dotted lines: $\overline{D}^*_{12}, \overline{D}^*_{21}$.

maximal value $0.56\overline{U}$, and the off-diagonal velocity elements decrease to $-0.28\overline{U}$ (see also section 7). For all γ the difference between $\overline{U}^0_{11}$ and $\overline{U}^0_{22}$ is at a maximum at about $\beta = 1$, where absolute values of $\overline{U}^*_{21}, \overline{U}^*_{12}$ reach their maxima.

Figure 5 shows the elements of the convective part of the effective diffusivity matrix. In the absence of coupling ($\gamma = 0$) the convective diffusivity decreases with Damkohler number from the value $\overline{U}^2 a^2/48D$ (at $\beta = 0$) to the value $0.06\overline{U}^2 a^2/48D$ (at $\beta \to \infty$). This effect of the surface reaction is explained by solute redistribution in favor of the region near the tube axis, where the velocity gradient is smaller.

Increasing molecular diffusivity D_c creates a more uniform cross-sectional distribution and, hence, tends to decrease the axial convective dispersion coefficient (see (2)). With increasing coupling ($D_c \to D$) molecular diffusivity $\delta_2 = D - D_c$ of the slow canonic component decreases, which promotes the corresponding dispersivity. This slow component governs the diagonal members $\overline{D}^*_{11} = \overline{D}^*_{22}$ of the dispersivity matrix, which also increases with increasing γ.

The coupling component of the molecular diffusivity provides an additional diffusive path for each species which also brings about a more uniform cross-sectional mass distribution. This effect is manifested by negative off-diagonal terms $\overline{D}^*_{12}, \overline{D}^*_{21}$, with concomitant reduction of the total diffusive flux (e.g. for the first component $\overline{D}^*_{11}\partial\overline{P}_1/\partial x + \overline{D}^*_{12}\partial\overline{P}_2/\partial x$). This effect is independent of the solute reactive properties. In particular, for $\beta = 0$ (both species are nonreactive) we obtain

$$\overline{\mathsf{U}}^* = \overline{U}\mathtt{I}, \quad \overline{\mathsf{D}}^* = \mathsf{D} + \frac{\overline{U}^2 a^2}{48}\mathsf{D}^{-1}, \tag{34a,b}$$

which generalizes the one-component formula (2a) of Taylor-Aris. One can directly verify that the off-diagonal terms of the matrix D^{-1} are negative.

For all γ the absolute values of all dispersivity elements decrease with increasing reactivity (growing β). This is explained by solute depletion from the wall vicinity due to chemical

reaction and the solute concentration redistribution in favor of the central region of the tube, where the flow velocity gradient (responsible for dispersion) is lower.

9. Discussion

In the presence of microscale molecular diffusion coupling, each solute component has two diffusive pathways to the wall (where it is destroyed by a surface reaction): one – via the direct diffusivity, another – via the coupling diffusivity. This gives rise to off-diagonal terms in the macroscopic matrix transport properties: positive coupling reactivities and negative coupling velocity and dispersivity elements. These coupling terms increase with increasing parameter γ. We will investigate the limiting forms of the transport coefficients when $\gamma \to 1$. Explicitly, we will look into circumstances, where

$$D = D_c + 2D', \quad 2D' \ll D, \tag{35}$$

so that $\delta_1 \approx 2D$, $\delta_2 \approx 2D'$. The strongest coupling prevails when the reactive parameters of the canonic components differ significantly, i.e.,

$$\beta_1 = Ga/2D \ll 1, \quad \beta_2 = Ga/2D' \gg 1. \tag{36a,b}$$

In this case we obtain

$$f_K(\beta_1) \approx 2\beta_1, f_K(\beta_2) \approx f_K(\infty) = 5.784, \tag{37a}$$

$$f_U(\beta_1) \approx 1, \quad f_U(\beta_2) \approx f_U(\infty) = 1.562, \tag{37b}$$

$$f_D(\beta_1) \approx 1, \quad f_D(\beta_2) \approx f_D(\infty) = 0.0576. \tag{37c}$$

Using the above, we can apply the inverse transformation (27) to (33a–c) to obtain

$$\overline{\mathsf{K}}^* = \frac{G}{a}\begin{bmatrix} 1 + 5.784D'/Ga & 1 - 5.784D'/Ga \\ 1 - 5.784D'/Ga & 1 + 5.784D'/Ga \end{bmatrix}, \tag{38a}$$

$$\overline{\mathsf{U}}^* = \overline{U}\begin{bmatrix} 1.2812 & -0.2812 \\ -0.2812 & 1.2812 \end{bmatrix}, \tag{38b}$$

$$\overline{\mathsf{D}}^* = \mathsf{D} + \frac{\overline{U}^2 a^2}{192D}\begin{bmatrix} 1 + 0.0576D/D' & 1 - 0.0576D/D' \\ 1 - 0.0576D/D' & 1 + 0.0576D/D' \end{bmatrix}. \tag{38c}$$

The reactivities of the canonic components are

$$\overline{K}_1^{\mathrm{o}} = 2G/a, \quad \overline{K}_2^{\mathrm{o}} = 5.784D'/a^2,$$

which means that in the present case characterized by (36) the fast (first) component is the most reactive ($\overline{K}_1^{\mathrm{o}} \gg \overline{K}_2^{\mathrm{o}}$). We will discuss the behavior of coefficients (38a–c) when the ratio D'/D approaches zero (with $D = \mathrm{const}$), in which limit the microscale diffusivity approaches the following singular matrix

$$D\begin{bmatrix} 1 & 1 \\ 1 & 1 \end{bmatrix}.$$

We can see that in this limit the effective reactivity matrix also degenerates, i.e., approaches a matrix with all identical elements, close to G/a, as determined by the largest reactivity $\overline{K}_1^{\circ}$ of the fastest canonic component [see (33a) and (36a,b)]. The difference between the values of the coupling and diagonal terms of $\overline{\mathsf{K}}^*$ are of the order $11.57\beta_2^{-1} \ll 1$. The degree of nonsingularity of $\overline{\mathsf{K}}^*$ depends upon the Damkohler number β_2 of the less reactive (slowest) canonic component.

The coarse-scale velocity matrix in the limit $D'/D \to 0$ is not singular, at least in circumstances when (35)–(36) are valid. In the case characterized by (36a,b), where the dimensionless canonic reactivities are different, the canonic components are transported with effective velocities which differ by about 56%. This results in the velocity matrix with off-diagonal elements having minimal value $-0.28\overline{U}$.

The ratio D'/D determines the sign of the coupling component of the axial dispersivity matrix. In particular, in the case where $D'/D < 0.0576$ the off-diagonal elements of $\overline{\mathsf{D}}^*$ are negative. In the limit $D'/D \to 0$ the coarse-scale diffusivity matrix tends to

$$\overline{\mathsf{D}}^* = 0.0288\,\frac{\overline{U}^2 a^2}{96D'}\begin{bmatrix} 1 & -1 \\ -1 & 1 \end{bmatrix} + \mathsf{D}, \tag{39}$$

which is also a singular matrix.

In the above we have considered the case where the macroscale velocities of each solute are equal (see section 6.2). In these circumstances, we may obtain from (18) that $\mathsf{Q} = \overline{U}\mathtt{I}$ and, hence, the second matrix term in the right-hand side of (23c) of the coarse-scale diffusivity is zero. In the case where the species experience a certain (e.g., gravitational) force, possessing nonzero component(s) perpendicular to the flow direction, the coarse-scale velocity matrix contains nonzero off-diagonal elements.

We will finally note that in the example considered here the effective coarse-scale equation (15) is reduced to the one-dimensional form (in terms of $x - t$ variables). Its solution may be obtained by standard methods at least for the steady problem formulation [43].

Acknowledgement

M.S. kindly acknowledges partial financial support of the Conseil Régional de la Région Poitou-Charentes during his sabbatical stay at LPTM/CNRS. This work has been partially supported by ANDRA.

Appendix A. Matrix eigenvalue problems

The problem posed for the zero-order moment by Equation (10a) ($m = 0$), subject to the boundary conditions (10b), (11a), may be treated by the method of separation of variables in its matrix form. Introduce solution (12) to the above problem posed for P_0, to obtain the following eigenvalue problems (EVPs) for column- and row-matrix functions $\mathsf{W}_k^{\backprime}(\mathbf{r}), \mathsf{A}_k^{\prime}(\mathbf{r})$ and the scalar eigenvalues λ_k; namely, the characteristic EVP

$$\mathsf{L}\mathsf{W}^{\backprime} = -\mathsf{W}^{\backprime}\lambda \quad \text{in} \quad \mathbf{r}_f, \tag{A1a}$$

$$\mathsf{S} = 0^{\backprime} \quad \text{on } s_p, \quad \mathsf{W}^{\backprime} - \text{periodic}, \tag{A1b,c}$$

and the adjoint EVP

$$\mathsf{L}_{\mathsf{A}}\mathsf{A}^{\backprime} \equiv \nabla\mathsf{A}^{\backprime}\cdot\mathbf{U}(\mathbf{r}) + \nabla\cdot(\nabla\mathsf{A}^{\backprime}\cdot\mathbf{D}(\mathbf{r})) = -\mathsf{A}^{\backprime}\lambda^* \quad \text{in } \mathbf{r}_f, \tag{A2a}$$

$$\mathsf{S}_{\mathsf{A}}\mathsf{A}' \equiv \mathbf{n}\cdot\nabla\mathsf{A}'\cdot\mathbf{D}(\mathbf{r}) + \mathsf{A}'\mathsf{G}(\mathbf{r}) = 0' \quad \text{on} \quad s_p, \quad \mathsf{A}' - \text{periodic.} \tag{A2b,c}$$

For any two-column matrix functions A', W' defined in $\mathbf{r}_f$, which, respectively, satisfy boundary conditions (A2b,c) and (A1b,c), we may show that

$$\langle \mathsf{A}', \mathsf{L}\mathsf{W}'\rangle = \langle \mathsf{L}_{\mathsf{A}}\mathsf{A}', \mathsf{L}\mathsf{W}'\rangle \tag{A3}$$

where the inner produce $\langle \ldots, \ldots\rangle$ of two (generally polyadic-valued) matrix functions, defined within $\mathbf{r}_f$, is given by the following relation:

$$\langle \mathsf{A}', \mathsf{W}'\rangle = \int_{\mathbf{r}_f} \mathsf{A}'(\mathbf{r})\mathsf{W}'(\mathbf{r})\,\mathrm{d}^3\mathbf{r}. \tag{A4}$$

We will assume that both of these EVPs possess solutions $\{\mathsf{A}'_k, \lambda^*_k\}\{\mathsf{W}'_k, \lambda_k\}(k = 1, 2, \ldots)$, characterized by discrete spectra. In these circumstances we may show [27] that both λ^*_k and λ_k consist of complex conjugate pairs and also $\lambda^*_k = \lambda_k, k = 1, 2, \ldots$.

Other eigenvalues may generally be complex, although we will be further interested in circumstances where at least the first n consecutive smallest eigenvalues are real. Sufficient conditions for this requirement may be outlined in each specific application of the general theory considered here, at least in cases where the matrices $\mathbf{D}$ and G are symmetric. For $\mathbf{D}$ the latter property is normally fulfilled, since it follows from the general Onsager relationships used in the irreversible thermodynamics [13].

Knowledge of the leading eigenvalue λ_1 appears to be of particular interest, since it represents the asymptotic long-time decay of the total masses (probabilities) of those species, the microscale transports of which are strongly coupled (see section 3).

Bearing in mind the adjointness property (A3) and the fact that the eigensolutions are each determined to within an arbitrary constant multiplier, we may show that they can be chosen to form biorthonormal sets $\{\mathsf{W}'_k\}, \{\mathsf{A}'\}$ in the sense that

$$\langle \mathsf{A}'_k, \mathsf{W}'_m\rangle = \delta_{km}. \tag{A5}$$

We will enumerate the eigensolutions in the order of increasing real parts of their eigenvalues, $\mathrm{Re}(\lambda_1) < \mathrm{Re}(\lambda_2) < \ldots$.

An alternative representation of the eigensolutions is via the square-matrix functions

$$\mathsf{W}_k \equiv [\mathsf{W}'_k\mathsf{W}'_{k+1}\ldots\mathsf{W}'_{k+n-1}], \mathsf{A}_k \equiv [A'^{\dagger}_k A'^{\dagger}_{k+1}\ldots A'^{\dagger}_{k+n-1}]^{\dagger}, \tag{A6a,b}$$

$(k = 1, n+1, 2n+1, \ldots)$, formed by n subsequent column and row-matrix eigenfunctions. We can easily show that $\mathsf{W}_k(\mathbf{r}), \mathsf{A}_k(\mathbf{r})$ satisfy the following EVPs (cf., (A1), (A2)):

$$\mathsf{L}\mathsf{W}_k = -\mathsf{W}_k\Lambda_k \quad \text{in} \quad \mathbf{r}_f, \quad \mathsf{S}\mathsf{W}_k = 0 \quad \text{on} \quad s_p, \quad \mathsf{W} - \text{periodic}, \tag{A7a,b,c}$$

$$\mathsf{L}_{\mathsf{A}}\mathsf{A}_k = -\Lambda_k\mathsf{A}_k \quad \text{in} \quad \mathbf{r}_f, \quad \mathsf{S}_{\mathsf{A}}\mathsf{A}_k = 0 \quad \text{on} \quad s_p, \quad \mathsf{A} - \text{periodic}, \tag{A8a,b,c}$$

where Λ_k is the eigenvalue matrix

$$\Lambda_k = \mathrm{Diag}[\lambda_k\lambda_{k+1}\cdots\lambda_{k+n-1}]. \tag{A9}$$

We may further verify that the sets $\{\mathsf{W}_k\}, \{\mathsf{A}_k\}$ composed from column- and row-matrix eigensolutions, biorthonormalized in accordance with (A5), are also biorthonormal, i.e.,

$$\langle \mathsf{A}_k, \mathsf{W}_m\rangle = \mathtt{I}\delta_{km}. \tag{A10}$$

We will also use the following identity

$$\langle \mathsf{Y}, \mathsf{LX}\rangle - \langle \mathsf{L}_{\mathsf{A}}\mathsf{Y}, \mathsf{X}\rangle = -\int_{\partial \mathbf{r}_0} \mathrm{d}^2\mathbf{s}\cdot(\mathsf{Y}\mathbf{j}\mathsf{X} + \nabla \mathsf{Y}\cdot\mathbf{D}\mathsf{X}), \tag{A11}$$

valid for any two polyadic-valued square-matrix functions Y, X, satisfying boundary conditions (A8b) and (A7b), respectively.

In the following we consider how the basic eigenvalue problems simplify in several particular cases.

Nonreactive species, i.e., $\mathsf{G}(\mathbf{r}) = \mathsf{0}$. We can see that the adjoint EVP (A2) has the following n-row matrix eigensolution

$$\lambda_1 = 0, \quad \mathsf{A}_1^{\backprime} = \mathtt{I}_{(k)} = [0 \quad 0\ldots 1\ldots 0], \quad k = 1, 2, \ldots, n, \tag{A12}$$

with unity appearing in the k-th place of the row matrix. Therefore, eigenvalue $\lambda_1 = 0$ is of multiplicity n. Corresponding (properly normalized) eigensolutions $\mathsf{W}_{1(k)}^{\backprime}(\mathbf{r}), k = 1, 2, \ldots, n$, represent the asymptotic, time-independent species concentrations, respectively, resulting from the initial distributions $\mathtt{I}_{(k)}, k = 1, 2, \ldots, n$. Each of these solutions may be interpreted as a long-time system response to the introduction of a nonreactive tracer particle in the corresponding k-th species. Noting that in this case $\mathsf{A}_1 = \mathtt{I}$ and bearing in mind (A10) with $k = m = 1$, we can rewrite the zero-order moment (8b) in the form

$$\mathsf{M}_0(t|\mathbf{r}') = \int_{\delta_f} \mathsf{W}_1(\mathbf{r})\,\mathrm{d}^3\delta = \langle \mathsf{A}_1, \mathsf{W}_1(\mathbf{r})\rangle = \overline{\mathsf{W}}_1 = \mathtt{I}, \tag{A13}$$

which is valid for all times $t > 0$. The eigensolutions

$$\mathsf{W}_1(\mathbf{r}), \quad \mathsf{A}_1(\mathbf{r}) = \mathtt{I}, \quad \Lambda_1 = \mathsf{0} \tag{A14a,b,c}$$

clearly satisfy the corresponding EVPs (A7), (A8). Therefore, in the absence of reactions, the solute mass on the coarse scale is equally distributed between the species, i.e., the solute partition matrix $\overline{\mathsf{W}}_1$ is the unity matrix, even in the presence of interstitial coupling, embodied in $\mathsf{W}_1(\mathbf{r})$.

Absence of convection. This is the case where $\mathbf{U}(\mathbf{r}) = \mathbf{0}$. We can see that, if $\mathbf{D}$ is a symmetric matrix, each of the basic EVPs (A1)–(A2) is self-adjoint. Then, we can normalize the eigenfunctions to have

$$\mathsf{W}_1 = \mathsf{A}_1^{\dagger}. \tag{A15}$$

Appendix B. Long-time solutions for first- and second-order moments

Introduce the trial solution (17) in the problem (10a,b) with $m = 1$, (11b), posed for $\mathbf{P}_1$ to obtain

$$\mathsf{L}\mathbf{B} + \mathbf{B}\Lambda_1 = \mathsf{W}_1(\mathbf{r})\mathbf{Q} \quad \mathbf{r} \in \mathbf{r}_f, \tag{B1}$$

$$\mathsf{S}\mathbf{B} = 0 \quad \text{on} \quad s_p, \quad [|\mathbf{B}|] = -\mathsf{W}_1[|\mathbf{r}|], \quad [|\nabla\mathbf{B}|] = -\nabla\mathsf{W}_1[|\mathbf{r}|]. \tag{B2a,b,c}$$

Solution for the $\mathbf{B}$ field may be constructed in the form

$$\mathbf{B}(\mathbf{r}) = \sum_k \mathsf{W}_k(\mathbf{r})\mathbf{C}_k. \tag{B3}$$

To obtain the constant vector-valued coefficients $\mathbf{C}_k = \langle \mathsf{A}_k, \mathbf{B}(\mathbf{r})\rangle (k = 1, 2, \ldots)$, appearing above, form the inner product (see (A4), (A10)) of both sides of (B3) with A_k. This yields

$$\langle \mathsf{A}_k, \mathsf{L}\mathbf{B}\rangle + \Lambda_k \mathbf{C}_k = \mathbf{Q}\delta_{k1}, \quad k = 1, 2, \ldots. \tag{B4}$$

The requisite value of $\mathbf{Q}$ is obtained from this equation for $k = 1$ and identity (A11), written with $\mathsf{Y} = \mathsf{A}_1, \mathsf{X} = \mathbf{B}$, which jointly yield

$$-\Lambda_1 \mathbf{C}_1 + \mathbf{C}_1 \Lambda_1 = \mathbf{Q} + \int_{\partial \mathbf{r}_o} \mathrm{d}^2\mathbf{s} \cdot (\mathsf{A}_1 \mathbf{j}\mathbf{B} + \nabla \mathsf{A}_1 \cdot \mathbf{D}\mathbf{B}). \tag{B5}$$

The left-hand side of this expression is a traceless matrix. Hence its right-hand side should have the same property. This provides an expression for $\mathbf{Q}$, which, with the help of boundary conditions (B2b,c), may be written in the form (18).

In circumstances, where Λ_1 is composed from different eigenvalues [36], the solution for the $\mathbf{B}$ field may be shown to be determined to within an additive term $\mathsf{W}_1(\mathbf{r})\mathbf{C}$ with $\mathbf{C}$ being an arbitrary constant vector-valued diagonal matrix. This property and the arbitrariness of the matrix $\mathbf{E}_1(\mathbf{r}')$ appearing in (17) may be shown to be without effect on the coarse-scale matrix transport coefficients.

The solution for the second-order moment is obtained by the introduction of trial form (19) into (10a,b) (with $m = 2$), (11c) and the use of (17), (B1)–(B2) to obtain the following problem for $\mathbf{H}$ field:

$$\mathsf{L}\mathbf{H} + \mathbf{H}\Lambda_1 = 2\mathsf{W}_1(\mathbf{r})\boldsymbol{\Delta} + 2[\mathbf{B}(\mathbf{r})\mathbf{Q}]^s \quad \text{in} \quad \mathbf{r}_f, \tag{B6}$$

$$\mathsf{S}\mathbf{H} = 0 \quad \text{on} \quad s_p, \quad [|\mathbf{H}|] = [|\mathbf{B}\mathsf{W}_1^{-1}\mathbf{B}|], \quad [|\nabla \mathbf{H}|] = [|\nabla(\mathbf{B}\mathsf{W}_1^{-1}\mathbf{B})|]. \tag{B7a,b,c}$$

In the above we have assumed that the matrix W_1 is nonsingular and, hence, its inverse W_1^{-1} exists.

The solution for problem (B6)–(B7) may be found in the form of eigenfunction expansion of $\mathbf{H}$ in terms of W_m, similarly to the solution of problem (B1)–(B2) for the $\mathbf{B}$ field. Using these arguments, we obtain expressions (20)–(21) for the required dyadic $\boldsymbol{\Delta}$. We may demonstrate that the value for $\boldsymbol{\Delta}$ is unaffected by the arbitrariness existing in the determination of the $\mathbf{B}$ field.

Note

* Address for correspondence

References

1. G.I. Taylor, Dispersion of soluble matter in solvent flowing slowly through a tube. *Proc. R. Soc. London* A219 (1953) 186–203.
2. R. Aris, On the dispersion of a solute in a fluid flowing through a tube. *Proc. Roy. Soc. London* A235 (1956) 67–77.
3. W.N. Gill and R. Sankarasubramanian, Dispersion of a nonuniform slug in a time-dependent flow. *Proc. Roy. Soc. London* A322 (1971) 101–117.
4. A.E. DeGance and L.E. Johns, The theory of dispersion of chemically active solutes in a rectilinear flow field. *Appl. Sci. Res.* 34 (1978) 189–225.
5. M. Shapiro and H. Brenner, Chemically reactive generalized Taylor dispersion phenomena. *AIChE Jour.* 33 (1987) 1155–1167.

6. M. Shapiro and H. Brenner, Taylor dispersion in the presence of time-periodic convection phenomena. Part II. Transport of transversely oscillating Brownian particles in a plane Poiseuille flow. *Phys. Fluids* A 2 (1990) 1744–1753.
7. R. Sankarasubramanian and W.N. Gill, Unsteady convective diffusion with interphase mass transfer. *Proc. Roy. Soc. London* A333 (1973) 115–132.
8. M. Shapiro and H. Brenner, Taylor dispersion of chemically reactive species: irreversible first-order reaction in bulk and on boundaries. *Chem. Eng. Sci.* 41 (1986) 1417–1433.
9. J. Dayan and O. Levenspeil, Longitudinal dispersion in packed beds of porous adsorbing walls. *Chem. Eng. Sci.* 23 (1968) 1327–1334.
10. H. Brenner, A. Nadim and S. Haber, Long-time molecular diffusion, sedimentation and Taylor dispersion of a fluctuating cluster of Brownian particles. *J. Fluid Mech.* 183 (1987) 511–542.
11. I. Frankel and H. Brenner, Taylor dispersion of orientable Brownian particles in unbounded homogeneous shear flows. *J. Fluid Mech.* 255 (1993) 129–156.
12. H. Brenner and D.A. Edwards, *Macrotransport Processes.* Boston: Butterworth-Heinemann (1993) 714 pp.
13. S.R. de Groot and P. Mazur, *Non-Equilibrium Thermodynamics*. Amsterdam: North Holland (1969) 510 pp.
14. E. Litovsky and M. Shapiro, Effective thermophysical properties of porous ceramic materials in wide ranges of temperature and gas pressure. Part 1. Dense ceramics with porosity below 30%. *J. American Ceramic Society* 75 (1992) 3425–3439.
15. T. Gambaryan, E. Litovsky and M. Shapiro, Influence of segregation-diffusion processes on the effective thermal conductivity of porous ceramics. *Int. journal of Heat and Mass Transfer* 36 (1993) 4123–4131.
16. O. Levenspiel, *Chemical Reaction Engineering* (2nd edn.). New York: Wiley (1972) 578 pp.
17. C.L. Carnahan, Non-equilibrium thermodynamics of groundwater flow systems: symmetry properties of phenomenological coefficients and considerations of hydrodynamic dispersion. *J. Hydrology* 31 (1976) 125–137.
18. C.R. Carrigan and R.T. Cygan, Implications of magma chamber dynamics for Soret-related fractionation. *J. Geophys. Res.* 91 (B11) (1986) 1451–1461.
19. J. Bear, *Dynamics of Flows in Porous Media.* New York: Dover (1988) 764 pp.
20. D.A. Edwards, M. Shapiro, H. Brenner and M. Shapira, Dispersion of inert solutes in spatially-periodic two-dimensional model porous media. *Transport in Porous Media* 6 (1991) 337–358.
21. G. Dagan, *Flow and Transport in Porous Formations*. New York: Springer-Verlag (1989) 465 pp.
22. M. Kaviany, *Principles of Heat Transfer in Porous Media*. New York: Springer-Verlag (1991) 626 pp.
23. P.M. Adler, *Porous Media. Geometry and Transports.* Boston: Butterworth-Heinemann (1992) 544 pp.
24. P.M. Adler, C.G. Jacquin and J.A. Quiblier, Flow in simulated porous media. *Int. J. Multiphase Flow* 16 (1990) 691–712.
25. J. Bensoussan, L. Lions and G. Papanicolau, *Asymptotic Analysis for Periodic Structures.* Amsterdam: North Holland (1978) 762 pp.
26. H. Brenner, Dispersion resulting from flow through spatially periodic porous media, *Phil. Trans. Roy. Soc. London* A297 (1980) 91–123.
27. M. Shapiro and H. Brenner, Dispersion of a chemically reactive solute in a spatially periodic model of a porous medium. *Chem. Eng. Sci.* 43 (1988) 551–571.
28. R. Mauri, Dispersion, convection and reaction in porous media. *Phys. Fluids* A3 (1991) 743–756.
29. D.A. Edwards, M. Shapiro and H. Brenner, Dispersion and reaction in two-dimensional model porous media. *Phys. Fluids* A5 (1993) 837–848.
30. P.M. Adler and H. Brenner, Dispersion resulting from flow through spatially periodic porous media. Surface and intraparticle transport. *Phil. Trans. Roy. Soc. London* A307 (1982) 149–200.
31. S.R. Dungan, M. Shapiro and H. Brenner, Convective-diffusive-reactive Taylor dispersion processes in particulate multiphase system *Proc. R. Soc. London* A429 (1990) 639–671.
32. L.H. Dill and H. Brenner, Dispersion resulting from flow through spatially periodic porous media – III. Time-periodic processes. *Physicochem Hydrodynam.* 4 (1983) 279–302.
33. G. Iosilevsky and H. Brenner, Taylor dispersion in systems containing a continuous distribution of reactive species. *Int. J. Non-linear Mech.* 28 (1993) 69–86.
34. T.A. Hatton and E.N. Lightfoot, Dispersion, mass transfer and chemical reaction in multiphase contactors. I: Theoretical developments. *AIChE J.* 30 (1984) 235–242. II: Numerical examples *AIChE J.* 30 (1984) 243–249.
35. A.E. DeGance and L.E. Johns, The theory of dispersion of the chemically active solutes in a rectilinear flow field: the vector problem. *Appl. Sci. Res.* 42 (1985) 55–88.
36. P. Lancaster and M. Tismenetsky, *The Theory of Matrices. Second Edition with Applications*. Orlando: Academic Press (1985) 570 pp.
37. I.C. Gohberg and M.G. Krein, *Introduction to the Theory of Linear Nonself-Adjoint Operators*. (Transl. of Mathematical Monographs, Vol. 18. Am. Math. Soc., Providence, RI, 1969) 378pp.

38. A.W. Naylor, G.R. Sell, *Linear Operator Theory in Engineering and Science*. New York: Springer-Verlag (1982) 624 pp.
39. M. Shapiro and H. Brenner, Convection and diffusion accompanied by bulk and surface chemical reactions in time-periodic one-dimensional flows. *SIAM J. Appl. Math.* 47 (1987) 1061–1075.
40. M. Shapiro and H. Brenner, Green's function formalism in generalized Taylor dispersion theory. *Chem. Engin. Commun.* 55 (1987) 19–27.
41. M. Shapiro, R. Fedou, J.-F. Thovert and P.M. Adler, Coupled transport and dispersion of multi-component reactive solutes in rectilinear flows. *Chem. Engin. Sci*. Accepted.
42. P. Spanne, J.F. Thovert, C.J. Jacquin, W.B. Lindquist, K.W. Jones and P.M. Adler., Synchrotron computed microtomography of porous media: Topology and transports. *Phys. Rev. Let.* 73 (1994) 2001–2004.
43. H.D. Do and D.D. Do, On the use of the characteristic method to solve linear homogeneous second-order differential equations with constant matrix coefficients for multicomponent reactive systems. *Chem. Eng. Sci*. 47 (1992) 2100–2102.